

See discussions, stats, and author profiles for this publication at: <https://www.researchgate.net/publication/49715349>

Magnetic Field-Induced Switching of the Radical-Pair Intersystem Crossing Mechanism in a Donor-Bridge-Acceptor Molecule for Artificial Photosynthesis

ARTICLE *in* JOURNAL OF THE AMERICAN CHEMICAL SOCIETY · FEBRUARY 2011

Impact Factor: 12.11 · DOI: 10.1021/ja1094815 · Source: PubMed

CITATIONS

27

READS

23

7 AUTHORS, INCLUDING:



Amy M Scott

Columbia University

19 PUBLICATIONS 545 CITATIONS

SEE PROFILE



Raanan Carmielli

Weizmann Institute of Science

44 PUBLICATIONS 877 CITATIONS

SEE PROFILE

Magnetic Field-Induced Switching of the Radical-Pair Intersystem Crossing Mechanism in a Donor–Bridge–Acceptor Molecule for Artificial Photosynthesis

Michael T. Colvin, Annie Butler Ricks, Amy M. Scott, Amanda L. Smeigh, Raanan Carmieli, Tomoaki Miura, and Michael R. Wasielewski*

Department of Chemistry and Argonne-Northwestern Solar Energy Research (ANSER) Center Northwestern University, Evanston, Illinois 60208-3113, United States

S Supporting Information

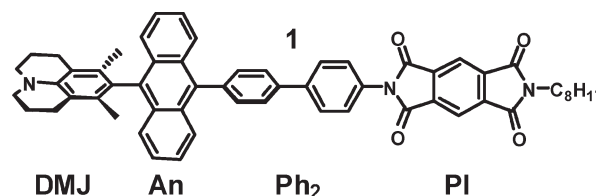
ABSTRACT: A covalent, fixed-distance donor–bridge–acceptor (D–B–A) molecule was synthesized that upon photoexcitation undergoes ultrafast charge separation to yield a radical ion pair (RP) in which the spin–spin exchange interaction ($2J$) between the two radicals is sufficiently large to result in preferential RP intersystem crossing to the highest-energy RP eigenstate (T_{+1}) at the 350 mT magnetic field characteristic of X-band (9.5 GHz) EPR spectroscopy. This behavior is unprecedented in covalent D–B–A molecules, and is evidenced by the time-resolved EPR (TREPR) spectrum at X-band of $^3\text{D}^+\text{--B--A}^-$ derived from RP recombination, which shows all six canonical EPR transitions polarized in emission (e,e,e,e,e,e). In contrast, when the RP is photogenerated in a 3400 mT magnetic field, the TREPR triplet spectrum at W-band (94 GHz) of $^3\text{D}^+\text{--B--A}^-$ displays the (a,e,e,a,a,e) polarization pattern characteristic of a weakly coupled RP precursor, similar to that observed in photosynthetic reaction center proteins, and indicates a switch to selective population of the lower-energy T_0 eigenstate.

One of the continuing challenges in developing molecular systems for artificial photosynthesis is the creation of long-lived charge-separated states.¹ Studies of competitive charge recombination accompanied by triplet state formation within donor–bridge–acceptor (D–B–A) molecules can provide a deeper understanding of how to minimize these energy-wasting processes. While time-resolved optical spectroscopy is often used to determine charge separation and recombination rates, time-resolved electron paramagnetic resonance (TREPR) spectroscopy can determine the spin-selective formation and decay mechanisms of radical ion pairs (RPs) and triplet states by monitoring their spin dynamics directly.

Following subnanosecond charge separation, the initially formed singlet (S) RP, $^1(\text{D}^{+\bullet}\text{--B--A}^{-\bullet})$, may undergo radical-pair intersystem crossing (RP-ISC)² to produce a triplet RP, $^3(\text{D}^{+\bullet}\text{--B--A}^{-\bullet})$. At the 350 mT magnetic field characteristic of TREPR spectroscopy at X-band (9.5 GHz), the $^3(\text{D}^{+\bullet}\text{--B--A}^{-\bullet})$ triplet sublevels are split by the Zeeman interaction (Figure 1), and are best described by the T_{+1} , T_0 , and T_{-1} eigenstates that are quantized along the applied magnetic field.³ When RP distances

are $< \sim 15 \text{ \AA}$, the RP singlet–triplet splitting, $2J$, which depends exponentially on distance, is generally large ($> 100 \text{ mT}$), so that the S and T_{+1} ($2J > 0$) or S and T_{-1} ($2J < 0$) spin states of the RP may be close in energy at high magnetic fields and mix. This situation is relatively rare, and has only been observed for a small number of diffusive RP encounters.⁴ The more typical case is one in which the RP distance is large and $2J$ is very small, resulting in S– T_0 mixing, as was originally observed in photosynthetic reaction center proteins,⁵ later in micellar systems,^{2a} and more recently in a variety of fixed distance D–B–A systems.^{3,6}

The subsequent charge recombination process is also spin selective; i.e. $^1(\text{D}^{+\bullet}\text{--B--A}^{-\bullet})$ recombines to the singlet ground state, while $^3(\text{D}^{+\bullet}\text{--B--A}^{-\bullet})$ recombines to yield the neutral triplet $^3(\text{D--B--A})$, which acquires the non-Boltzmann spin population of the triplet RP state.⁷ The spin polarization pattern of the six EPR transitions of $^3(\text{D--B--A})$ at the canonical (x,y,z) orientations relative to the applied magnetic field can be used to differentiate its formation mechanism from the ordinary spin–orbit intersystem crossing mechanism. For example, when a RP undergoes ISC by S– T_n mixing, where the degree of mixing is in the order $T_{+1} > T_0 \gg T_{-1}$, the subsequent charge recombination to the neutral triplet yields a (e,e,e,e,e,e) polarization pattern (low field to high field), while S– T_0 mixing alone yields an (a,e,e,a,a,e) pattern.⁷



We have prepared a D–B–A system consisting of a 3, 5-dimethyl-4-(9-anthracenyl)-julolidine (DMJ–An) donor, and a pyromellitimide (PI) acceptor connected by a biphenyl bridge (Ph₂), **1**. The synthesis and characterization of **1** is detailed in the Supporting Information, while the excited state and redox properties of DMJ–An and PI, respectively, have been described previously.^{6,8} Photoexcitation of **1** in toluene at 416 nm results in formation of $^1(\text{DMJ}^{+\bullet}\text{--An--Ph}_2\text{--PI}^{-\bullet})$ as indicated by the appearance of a strong 720 nm $\text{PI}^{-\bullet}$ absorption band⁸ with

Received: October 21, 2010

Published: December 30, 2010

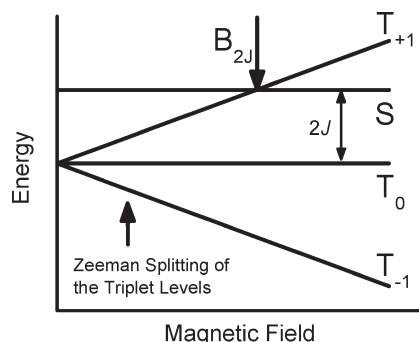


Figure 1. Schematic of radical ion pair energy levels as a function of magnetic field ($2J > 0$).

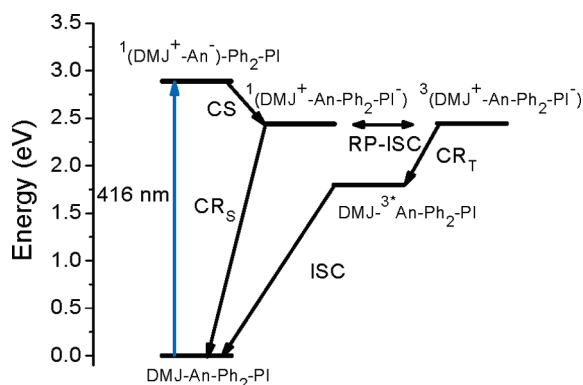


Figure 2. Energies and photophysical pathways for **1**.

$\tau_{CS} = 9 \pm 1$ ps (Figure S2, Supporting Information [SI]). The relevant excited state and RP energies are given in Figure 2, while the RP distances are given in Table S1 (SI). Nanosecond transient absorption spectroscopy at 295 K shows that charge recombination occurs with $\tau_{CR} = 40 \pm 1$ ns, followed by the appearance of $^3^*An$ at 430 nm (Figure 3).⁹

As noted above, application of a static magnetic field causes Zeeman splitting of the RP triplet sublevels, and varying the field strength modulates the efficiency of RP-ISC by adjusting the $T_{\pm 1}$ triplet sublevel energies relative to that of the singlet level (Figure 1). When the Zeeman splitting of the triplet radical pair sublevels equals $2J$, there is an increase in the RP-ISC efficiency. This increase translates into a maximum in triplet RP production and therefore a maximum in the neutral triplet yield upon charge recombination, so that $2J$ can be measured directly by monitoring the resonance in the neutral triplet yield as a function of applied magnetic field.¹⁰ The mechanistic details of RP-ISC and the theory behind magnetic field effects (MFEs) on reaction yields have been described previously^{2,11} and applied to donor–acceptor systems.¹² For **1**, $2J = 210 \pm 10$ mT at 295 K (inset, Figure 3).

Since the TREPR observations of $DMJ-^3^*An-Ph_2-PI$ following charge recombination described below are carried out at low temperatures in a glassy solvent and previous work has shown that $2J$ decreases in D–B–A molecules in which B is a *p*-phenylene oligomer due largely to restricted torsional motions, the MFE on the RP yield of **1** in 2-methyltetrahydrofuran (2-MTHF) was measured at 80 K (Figures 4 and S4 [SI]). The decay of $DMJ^{+*}-An-Ph_2-PI^{-*}$ monitored at 720 nm and 80 K is multiphasic with a principal decay time of $\tau = 523 \pm 54$ ns (Figure S4 [SI]) and $2J = 130 \pm 20$ mT (Figure 4). The MFE is monitored at

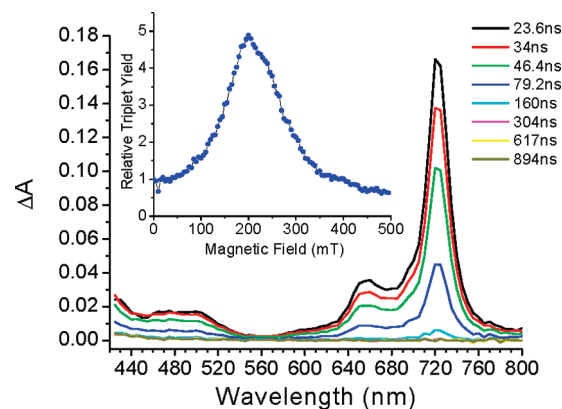


Figure 3. Nanosecond transient absorption of **1** at times indicated following a 7 ns 416 nm laser pulse. Inset: MFE monitored at 440 nm 1 μ s after the laser pulse.

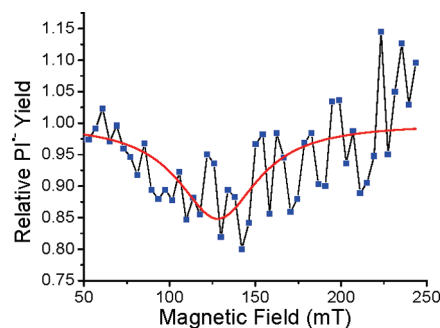


Figure 4. MFE of **1** monitored by transient absorption at 720 nm and 70 ns after a 7 ns, 416 nm laser pulse at 80 K in 2-MTHF.

720 nm where PI^{-*} has an intense absorption because the signal-to-noise ratio is superior compared to that when monitoring $^3^*An$. Thus, $2J$ remains relatively large, even at low temperatures. Unfortunately, **1** is only sparingly soluble in 2-MTHF, which prevents making samples at concentrations sufficiently large to obtain high-quality TREPR spectra. Nevertheless, the dielectric constants for most frozen organic solvents at low temperatures are very similar, so that ΔG and the reorganization energy for charge recombination should be similar in both 2-MTHF and toluene, the solvent in which the TREPR spectra of **1** are obtained.¹³

In order to elucidate the mechanism by which $^3^*An$ is formed upon charge recombination within **1**, TREPR spectra were acquired at 85 K at both X- and W-bands and are shown in Figure 5. The spectra were simulated with a home-written MATLAB¹⁴ program using published models.^{5b} The observed triplet spectrum was simulated with a D value of 71.9 mT and an E value of -8.1 mT, matching the reported $^3^*An$ D and E values.⁶ Unlike previously observed triplet state TREPR spectra, the polarization pattern shows all six transitions in emission at X-band. The absolute phase of the spectrum was verified using the stable free radical α,γ -bis(diphenylene)- β -phenylallyl (BDPA) as a standard.

The emissive transitions indicate that there is substantial overpopulation of the T_{+1} sublevel. However, since six transitions were observed and double quantum transitions are forbidden, the population must be distributed between the T_{+1} and T_0 sublevels. Additionally, the TREPR spectrum at X-band is not symmetric, indicating that the population difference is not equally distributed between T_{+1} and T_0 . The intensity of the transitions is proportional

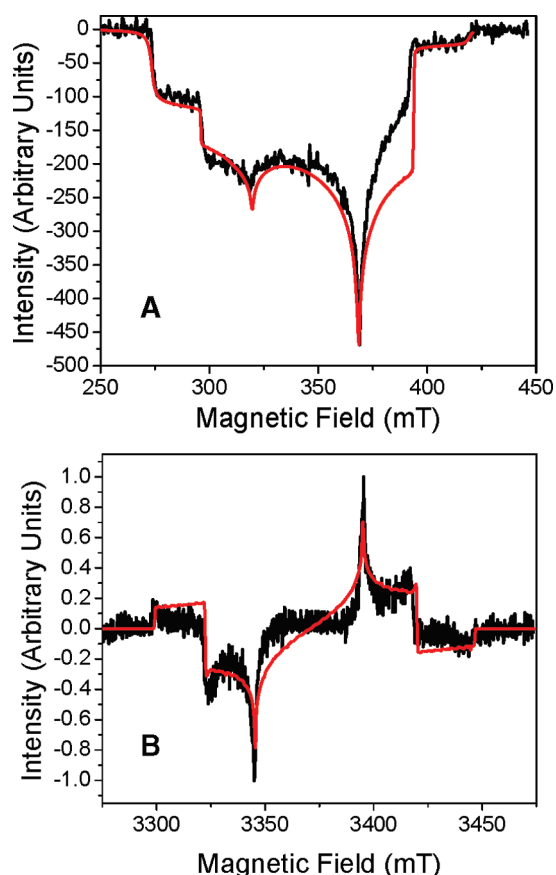


Figure 5. TREPR spectra of **1** (a) at X-band in toluene at 85 K, 150 ns after a 7 ns, 416 nm laser pulse, and (b) at W-band in toluene at 85 K, 2 μ s after a 7 ns, 416 nm laser pulse. Simulations are shown in red.

to the population difference between the different sublevels (Figure 6A). The degree of $S-T_n$ mixing is directly proportional to the matrix elements that couple S and T_n and inversely proportional to the energy gap between them.^{4c} At 350 mT, the $S-T_{+1}$ energy gap is comparable to that of the $S-T_0$ energy gap, allowing for mixing of S with both T_0 and T_{+1} . If mixing was dominated by the energy gap, a greater population in the T_0 sublevel of ^3An would be observed. Therefore, the data indicate that the matrix element coupling S and T_{+1} is primarily responsible for the majority population residing initially on T_{+1} . Although we did not observe the RP directly by TREPR spectroscopy, the population of the neutral triplet state should reflect that of its RP precursor because charge recombination is spin selective.¹⁵

To investigate the magnetic field dependence of RP-ISC in **1** we acquired the TREPR spectrum of its triplet state following RP recombination at W-band (94 GHz, 3400 mT) (Figure 5B). The W-band spectrum shows a triplet-state spectrum with the same D and E values (± 2.5 mT) as for the one observed at X-band, given the lower signal-to-noise ratio at W-band, but having an (a, e, e, a, a, e) polarization pattern indicative of selective T_0 overpopulation (Figure 6B).¹⁵ This is a result of the ~ 10 -fold increase in the magnetic field, which makes the Zeeman splitting much greater than $2J$ and therefore prohibits mixing between the S and the T_{+1} sublevels of the RP, leaving only $S-T_0$ mixing to occur. The triplet state spectrum was best fit by a linear combination of radical pair and spin-orbit mechanisms with a ratio of 9:1, respectively. It is known that charge-transfer-induced spin-orbit ISC occurs in $1^+(\text{DMJ}-\text{An})$ as a result of the perpendicular geometry of the

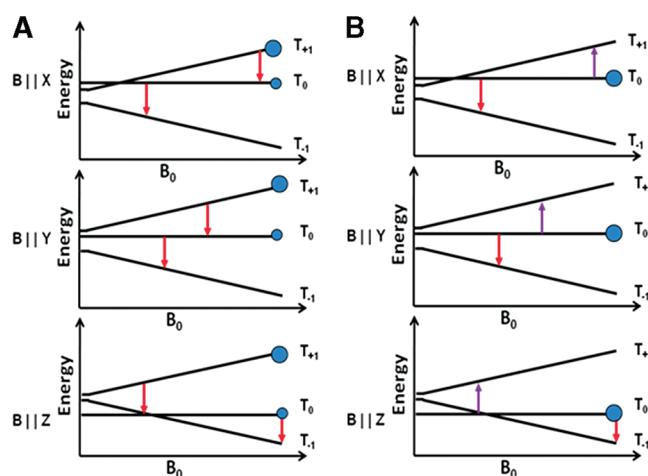


Figure 6. Schematic for EPR transitions in all three canonical orientations with (A) T_{+1} overpopulated and some population on T_0 sublevels and with (B) overpopulation on T_0 sublevel. Blue circles represent the population differences of the three triplet sublevels relative to the least populated sublevel, red arrows represent emissive transitions, and purple arrows represent absorptive transitions.

DMJ and An π systems.⁶ It is likely that the small spin-orbit ISC contribution observed results from $1^+(\text{DMJ}-\text{An}-\text{Ph}_2-\text{PI})$ molecules that do not fully charge separate at 80 K, as indicated by nanosecond transient absorption spectroscopy (Figure S4, [SI]). By taking the spin-orbit contribution into account, the X-band triplet simulation yields the population differences for the three triplet sublevels as 1: 0.20 ± 0.03 : 0 for T_{+1} : T_0 : T_{-1} , respectively, which is consistent with the observed (e, e, e, e, e) polarization pattern requiring that the triplet sublevels are populated preferentially in the order $T_{+1} > T_0 \gg T_{-1}$.

Using TREPR spectroscopy to monitor the change in triplet sublevels populated by RP-ISC as a function of magnetic field, we have shown that, when $2J$ is sufficiently large, RP-ISC in fixed distance D-B-A molecules can proceed through triplet sublevels other than T_0 . This demonstrates that triplet formation is still a viable charge recombination pathway even when the donor and acceptor are strongly coupled to one another and needs to be considered when designing D-B-A molecules for solar energy conversion applications.

■ ASSOCIATED CONTENT

S Supporting Information. Experimental details including the synthesis, transient absorption spectra and kinetics, and magnetic field effect data for **1**. This material is available free of charge via the Internet at <http://pubs.acs.org>.

■ AUTHOR INFORMATION

Corresponding Author
m-wasielewski@northwestern.edu

■ ACKNOWLEDGMENT

This work was supported by the Division of Chemical Sciences, Geosciences, and Biosciences, Office of Basic Energy Science, U.S. Department of Energy under Grant no. DE-FG02-99ER14999. M.T.C. thanks the Link Foundation for a fellowship.

■ REFERENCES

- (1) Wasielewski, M. R. *J. Org. Chem.* **2006**, *71*, 5051–5066.
- (2) (a) Closs, G. L.; Forbes, M. D. E.; Norris, J. R. *J. Phys. Chem.* **1987**, *91*, 3592–3599. (b) Hore, P. J.; Hunter, D. A.; McKie, C. D.; Hoff, A. J. *Chem. Phys. Lett.* **1987**, *137*, 495–500.
- (3) (a) Hasharoni, K.; Levanon, H.; Greenfield, S. R.; Gosztola, D. J.; Svec, W. A.; Wasielewski, M. R. *J. Am. Chem. Soc.* **1995**, *117*, 8055–8056. (b) Hasharoni, K.; Levanon, H.; Greenfield, S. R.; Gosztola, D. J.; Svec, W. A.; Wasielewski, M. R. *J. Am. Chem. Soc.* **1996**, *118*, 10228–10235. (c) Carbonera, D.; DiValentin, M.; Corvaja, C.; Agostini, G.; Giacometti, G.; Liddell, P. A.; Kuciauskas, D.; Moore, A. L.; Moore, T. A.; Gust, D. *J. Am. Chem. Soc.* **1998**, *120*, 4398–4405. (d) Kobori, Y.; Yamauchi, S.; Akiyama, K.; Tero-Kubota, S.; Imahori, H.; Fukuzumi, S.; Norris, J. R., Jr. *Proc. Natl. Acad. Sci. U.S.A.* **2005**, *102*, 10017–10022. (e) Dance, Z. E. X.; Mi, Q. X.; McCamant, D. W.; Ahrens, M. J.; Ratner, M. A.; Wasielewski, M. R. *J. Phys. Chem. B* **2006**, *110*, 25163–25173.
- (4) (a) Adrian, F. J.; Monchick, L. J. *Chem. Phys.* **1979**, *71*, 2600–2610. (b) Adrian, F. J.; Monchick, L. J. *Chem. Phys.* **1980**, *72*, 5786–5787. (c) Atkins, P. W.; Dobbs, A. J.; McLaughlan, K. A. *Chem. Phys. Lett.* **1973**, *22*, 209–211. (d) Honma, H.; Murai, H.; Kuwata, K. *Chem. Phys. Lett.* **1992**, *195*, 239–242. (e) Tominaga, K.; Yamauchi, S.; Hirota, N. *J. Chem. Phys.* **1988**, *88*, 553–562. (f) Trifunac, A. D.; Nelson, D. J.; Mottley, C. *J. Magn. Reson.* **1978**, *30*, 263–272. (g) Trifunac, A. D.; Nelson, D. J. *J. Am. Chem. Soc.* **1977**, *99*, 289–290.
- (5) (a) Dutton, P. L.; Leigh, J. S.; Seibert, M. *Biochem. Biophys. Res. Commun.* **1972**, *46*, 406–413. (b) Regev, A.; Nechushtai, R.; Levanon, H.; Thornber, J. P. *J. Phys. Chem.* **1989**, *93*, 2421–2426. (c) Rutherford, A. W.; Paterson, D. R.; Mullet, J. E. *Biochim. Biophys. Acta* **1981**, *635*, 205–215.
- (6) Dance, Z. E. X.; Ahrens, M. J.; Vega, A. M.; Ricks, A. B.; McCamant, D. W.; Ratner, M. A.; Wasielewski, M. R. *J. Am. Chem. Soc.* **2008**, *130*, 830–832.
- (7) Levanon, H.; Hasharoni, K. *Prog. React. Kinet.* **1995**, *20*, 309–346.
- (8) Gosztola, D.; Niemczyk, M. P.; Svec, W.; Lukas, A. S.; Wasielewski, M. R. *J. Phys. Chem. A* **2000**, *104*, 6545–6551.
- (9) Livingston, R.; Tanner, D. W. *Trans. Faraday Soc.* **1958**, *54*, 765–771.
- (10) (a) Anderson, P. W. *Phys. Rev.* **1959**, *115*, 2–13. (b) Shultz, D. A.; Fico, R. M., Jr.; Bodnar, S. H.; Kumar, R. K.; Vostrikova, K. E.; Kampf, J. W.; Boyle, P. D. *J. Am. Chem. Soc.* **2003**, *125*, 11761–11771.
- (11) (a) Weller, A.; Staerk, H.; Treichel, R. *Faraday Discuss. Chem. Soc.* **1984**, *78*, 271–278. (b) Hoff, A. J.; Gast, P.; van der Vos, R.; Franken, E. M.; Lous, E. J. *Z. Phys. Chem.* **1993**, *180*, 175–192. (c) Till, U.; Hore, P. J. *Mol. Phys.* **1997**, *90*, 289–296. (d) Steiner, U. E.; Ulrich, T. *Chem. Rev.* **1989**, *89*, 51–147.
- (12) (a) Sakaguchi, Y.; Hayashi, H. *J. Phys. Chem. A* **1997**, *101*, 549–555. (b) Tanimoto, Y.; Okada, N.; Itoh, M.; Iwai, K.; Sugioka, K.; Takemura, F.; Nakagaki, R.; Nagakura, S. *Chem. Phys. Lett.* **1987**, *136*, 42–46. (c) Werner, U.; Kuhnle, W.; Staerk, H. *J. Phys. Chem.* **1993**, *97*, 9280–9287.
- (13) Gaines, G. L., III; O'Neil, M. P.; Svec, W. A.; Niemczyk, M. P.; Wasielewski, M. R. *J. Am. Chem. Soc.* **1991**, *113*, 719–721.
- (14) MATLAB; The MathWorks, Inc.: Natick, MA, 2006.
- (15) Levanon, H.; Norris, J. R. *Chem. Rev.* **1978**, *78*, 185–198.